Reaction of Porous Solids

E. E. PETERSEN

University of California, Berkeley, California

A method is presented for the analysis of a reaction between a porous solid and a gaseous reactant where the kinetic expression is linear in the concentration and where appreciable concentration gradients are established in the pore system as a result of diffusive transport rate. Two cases are treated mathematically: a single cylindrical pore initially of uniform diameter and a porous solid initially containing uniform cylindrical pores with random intersections. The mathematical solutions to the latter case are used to interpret the experimental results reported in the literature on the gasification of graphite rods with carbon dioxide. Values of the computed effective diffusivity are an order of magnitude smaller than the bulk diffusivity at the same temperature and pressure.

Numerous heterogeneous reactions between a solid and a fluid phase have been studied, many of which are industrially important. In most instances it is desirable to increase the "reactivity" of the solid phase by dispersing it in a finely divided state or by developing a porous structure within the solid phase or by combinations of both in order to obtain a high specific surface area. In order to utilize the large surface area developed within solids, the reactant must be transported into the interior of the solid, where the major part of the reaction occurs, and the resultant products must be transported out. The important mechanism for transport is generally diffusion. However, solids with high specific surface areas are characterized by small pores, and appreciable concentration gradients are obtained in the pore system when the diffusive transport rates are large. These concentration gradients decrease the effectiveness for chemical reaction of each unit surface progressively more deeply within the interior of the solid. This paper is concerned with the quantitative description of the reaction between a porous solid and a fluid phase when concentration gradients occur within the pore system. Two cases will be considered: a single uniform pore and a porous cylindrical sample containing uniform cylindrical pores with random intersections.

Thiele (*7*) solved the analogous problem of heterogeneous reactions between porous catalysts and fluids in which the pore geometry of the solid phase was assumed to be independent of time. He solved the cases of uniform cylindrical pores for zero first and second order reactions and spheres with first order kinetics. The current literature on these systems is well summarized by Wheeler (*10*) and Weisz and Prator (*9*).

The unsteady state equation describing the simultaneous reaction and mass transport in a porous solid is

$$\frac{\partial C}{\partial t} = -\text{div}\,(-D\ \text{grad}\ C) - \text{div}\,(uC) - aR' \qquad (1)$$

where the terms on the right side of the equation refer to the diffusive transport, the convective transport, and a source or sink corresponding to chemical reaction The corresponding energy equation is not considered in this paper, as constant temperature is assumed throughout the solid phase. The radius of the pore is a function of position and time and appears in the divergence terms of Equation (1). Therefore, Equation (2) must be solved simultaneously with Equation (1).

$$\frac{\partial r}{\partial t} = \frac{M}{\rho_s} R' \qquad (2)$$

With the aid of Equations (1) and (2) the single-pore and cylindrical-rod cases will be considered individually. Each case will be subject to the following restrictions:

1. The convective term is dropped because the reaction yields no net change in number of moles or because the pore radii are so small that convective transport is small compared with diffusive transport.
2. The reaction is first order.
3. The pore walls are smooth. If the walls have a surface roughness σ, which is constant, the second term on the right becomes $(2\sigma kC)/r$.
4. The diffusivity is constant; therefore the equation does not apply in the Knudsen region for large changes in r.

All these restrictions can be removed, but the results tabulated in this paper are subject to the assumptions listed above.

SINGLE-PORE MODEL

A sketch of the single-pore model is shown in Figure 1. The initial pore is a long cylindrical pore of radius r_0 and length $2L$ where $L \gg r_0$. The concentration at either pore mouth is C_0 and constant. For this model Equation (1) becomes

$$\frac{\partial C}{\partial t} = \frac{D}{r^2}\frac{\partial}{\partial x}\left(r^2 \frac{\partial C}{\partial x}\right) - \frac{2}{r} kC \qquad (3)$$

Equations (2) and (3) can be put in dimensionless form:

$$\frac{\partial \psi}{\partial \tau} = \frac{1}{\xi^2}\frac{\partial}{\partial \eta}\left(\xi^2 \frac{\partial \psi}{\partial \eta}\right) - \alpha^2 \frac{\psi}{\xi} \qquad (4)$$

where

$$\xi = \frac{r}{r_0},\ \eta = \frac{x}{L},\ \psi = \frac{C}{C_0},\ \tau = \frac{Dt}{L^2},$$

and

$$\alpha = L\sqrt{\frac{2k}{r_0 D}}.$$

$$\frac{\partial \xi}{\partial \tau} = \frac{M}{2\rho_s}\alpha^2 C_0 \psi \qquad (5)$$

Equations (4) and (5) can be solved numerically, but in order to keep the solution stable an unreasonably large number of iterations would be required. However, it is apparent from the physical picture and can be justified mathematically* that, although an unsteady state solution to Equations (4) and (5) is required, the concentrations within the pore very rapidly approach a steady state profile; that is, before any significant amount of material is reacted from the pore wall the concentration profile has approached the steady state solution for a uniform pore of radius r_0. Then as material is removed from the pore walls, the concentration profile within the pore is almost exactly identical with the steady state profile. This simplification greatly reduces the time required to obtain solutions because Equation (4) is now an ordinary nonlinear differential equation and is solved numerically by computing the steady state concentration profile in the initial pore by Equation (6) below:

$$\frac{1d}{\xi^2 d\eta}\left(\xi^2 \frac{d\psi}{d\eta}\right) - \alpha^2 \frac{\psi}{\xi} = 0 \qquad (6)$$

The new pore-radius profile is computed from the concentration profile by use of Equation (5). The steady state concentration profile is then computed for the new pore-radius profile, and so on.

The problem now is to solve Equation (6) with boundary conditions:

$$\psi(0) = 1;\quad \left.\frac{d\psi}{d\eta}\right|_{\eta=1} = 0 \qquad (7)$$

This can be numerically handled very conveniently by matrix algebra. If the η coordinate is arbitrarily divided into m intervals where $m = 0$ is at the pore mouth, in finite-difference form Equation (6) can be expressed as

$$a_m\psi_{m+1} + b_m\psi_m + d_m\psi_{m-1} = 0 \qquad (8)$$

where m takes values of 1, 2, 3, $\cdots$ m and

$$a_m = 1 + \frac{\xi_{m+1} - \xi_{m-1}}{2\xi_m}$$

*See Appendix I.

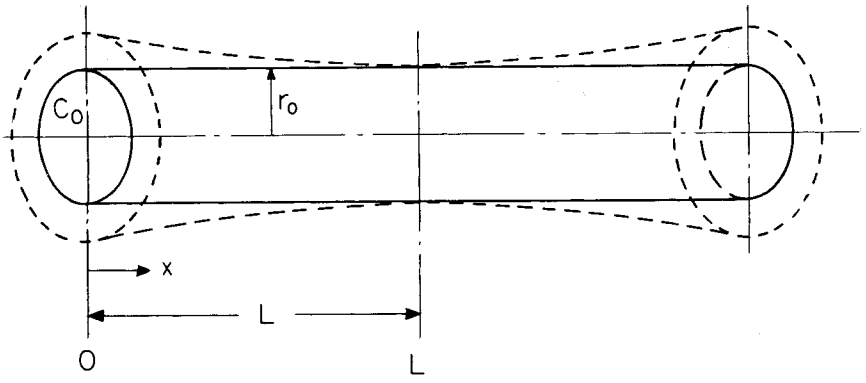

Fig. 1. Single-pore model.

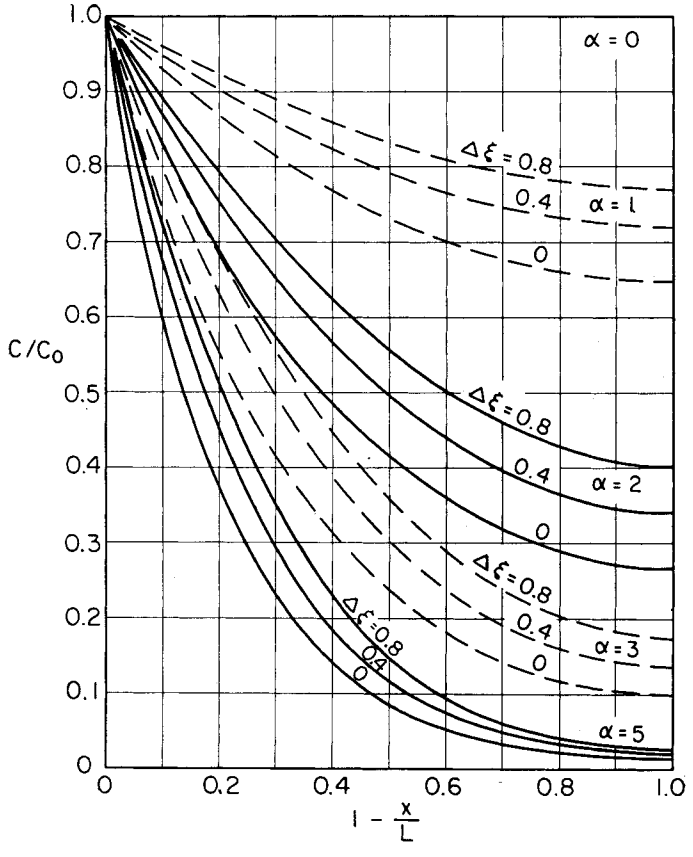

Fig. 2. Concentration profiles within single pore.

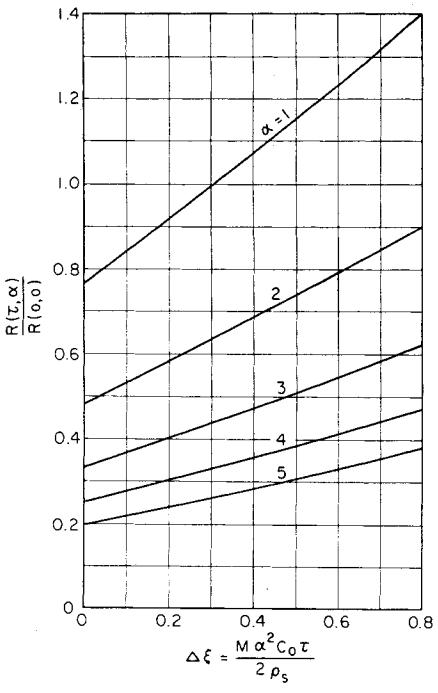

Fig. 3. Relative reaction rates as a function of time for various values of the parameter α for single-pore model.

$$(\psi) \equiv \begin{bmatrix} \psi_1 \\ \psi_2 \\ \psi_3 \\ \cdot \\ \cdot \\ \psi_m \end{bmatrix} \quad \text{and} \quad (B) \equiv \begin{bmatrix} -d_1 \\ 0 \\ 0 \\ 0 \\ \cdot \\ \cdot \end{bmatrix}$$

The solution to the equations above can be represented by Equation (10):

$$(\psi) = (A^{-1})(B) \qquad (10)$$

where (A^{-1}) is the inverse matrix of (A). The inversion for this particular case can be accomplished by the method of cofactors (3).

A finite-difference form of Equation (5) is given below:

$$\xi_{m,\tau+\Delta\tau} - \xi_{m,\tau} = \frac{M}{2\rho_s}\alpha^2 C_0 \psi \Delta\tau$$

$$= \Delta\xi_m$$

$$b_m = -\left[2 + \frac{\alpha^2 \Delta\eta^2}{\xi_m}\right]$$

$$d_m = 1 - \frac{\xi_{m+1} - \xi_{m-1}}{2\xi_m}$$

One has m equations given by Equation (8) and two boundary conditions of Equation (7) which can be written compactly in the matric equation below:

$$(A)(\psi) = (B) \qquad (9)$$

where

$$(A) \equiv \begin{bmatrix} b_1 & a_1 & 0 & 0 & 0\cdots & & & \\ d_2 & b_2 & a_2 & 0 & 0 & 0\cdots & & \\ 0 & d_3 & b_3 & a_3 & 0 & 0\cdots & & \\ 0 & 0 & d_4 & b_4 & a_4 & 0\cdots & & \\ \cdots & \cdots & \cdots & \cdots & \cdots & \cdots & \cdots & \cdots \\ & & \cdots 0 & 0 & d_{m-2} & b_{m-2} & a_{m-2} & 0 \\ & & \cdots 0 & 0 & 0 & d_{m-1} & b_{m-1} & a_{m-1} \\ & & \cdots 0 & 0 & 0 & 0 & a_m + d_m & b_m \end{bmatrix}$$

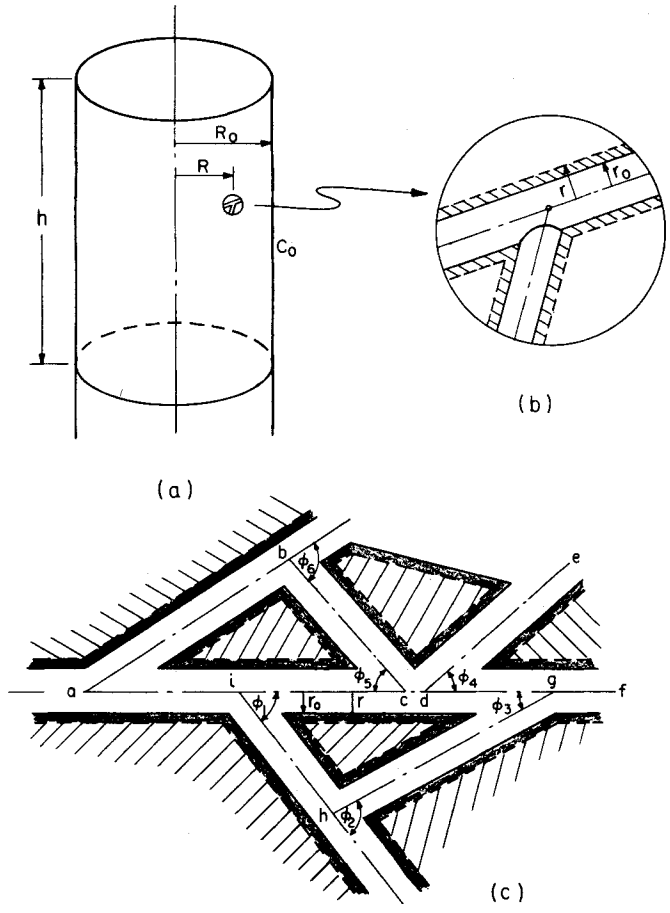

Fig. 4. Model of porous solid with random intersections.

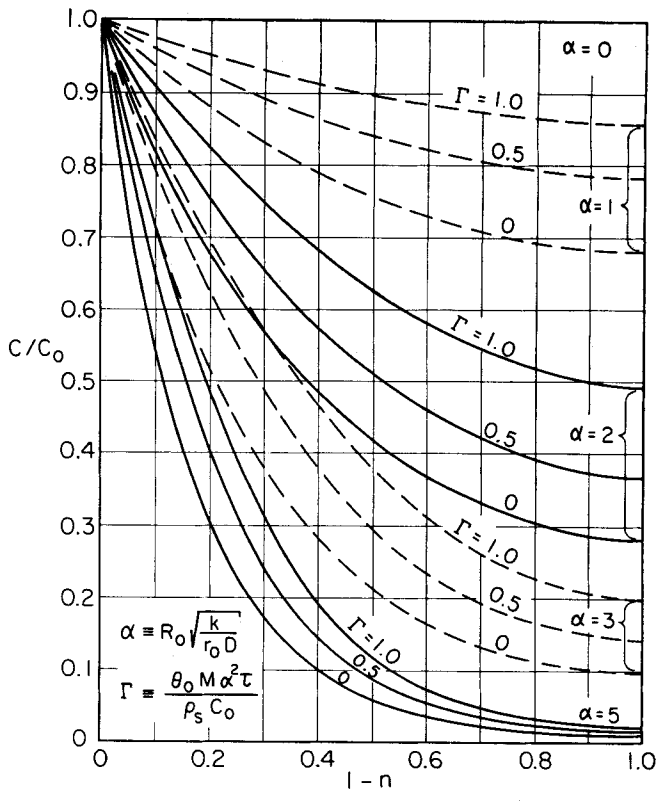

Fig. 5. Concentration profiles within porous-solid model.

If $\Delta\xi_0$ = the change in radius at the pore mouth in time τ, then

$$\frac{\Delta\xi_m}{\Delta\xi_0} = \frac{\psi_m}{\psi_0}$$

$$\Delta\xi_m = \left(\frac{\psi_m}{\psi_0}\right)\Delta\xi_m. \qquad (11)$$

The numerical computations were made on the IBM type 650 magnetic drum computer. The computer program made provision for changing the number of space and time intervals, the values of which were chosen so that the absolute error of the computed concentration profiles is within about 1%.

The results of these computations are shown in Figures 2 and 3. In Figure 2 the concentrations at various depths within the pore are shown. The concentration profiles for $\tau = 0$ are the same as given by Thiele (7). As the pore enlarges owing to reaction, the concentration progressively increases at points within the interior. The rates at which single pores react are shown in Figure 3. The ordinate is the ratio of the rate at which the pore reacts to that which would be obtained in the initial pore if the area of the pores was completely accessible at unit concentration. The abscissa is a dimensionless time obtained from Equation (5) and corresponds to the fractional change in pore radius at time τ. Again, the values at $\tau = 0$ correspond to the solutions obtained by Thiele (7).

The results of the single-pore model are useful in predicting general behavior; however, they do not possess certain characteristics of porous materials. For example, the rates in Figure 3 would continue to increase with time, whereas the rate of reaction of a porous solid would go through a maximum owing to the eventual decrease in the sample area as the sample disappears. To get this observed behavior a model must be used which considers every pore in the system and its spatial relation to other pores.

CYLINDRICAL PELLET MODEL

In a long cylindrical rod of radius R_0 and of length h, containing cylindrical pores initially of uniform radius r_0, intersecting each other randomly as shown in Figure 4, the dimensions of the solid are such that $h \gg R_0 \gg r_0$. If the structure of the solid is initially of uniform porosity θ_0 and the pores are distributed randomly throughout the solid, an arbitrary plane passed through the sample will have a fraction θ_0 corresponding to pores and the remainder $1 - \theta_0$ corresponding to solid, provided that the arbitrary plane is large enough to intersect a statistical number of pores. In order to solve Equation (1), a relationship between the pore radius r and the porosity θ must be obtained.

The required relationship between θ and r can be obtained by assuming that the differential volume used to develop Equation (1) can be represented by the idealized network of pores shown in Figure 4c. Since the concentration is constant, the pores increase from r_0 to r uniformly throughout the differential volume. The length of the pore system per unit volume L is defined as the sum of the center-line distances of the pores; i.e.,

$$L = ab + bc + cd + gh + \cdots$$

and N = the number of pore intersections per unit volume. If the pores enlarge uniformly, then the surface area of the smooth pores of radius r is given by

$$S = 2\pi r\left[L - r\sum_{i=1}^{N}\left(\frac{1}{\sin\phi_i}\right)\right] - r^2\sum_{i=1}^{N}\beta(\phi_i) \qquad (12)$$

where the second term on the right accounts for the area of the openings in the pore walls and $\beta(\phi_i)$ is a shape factor of the ith intersection based on the angle ϕ_i. The term

$$\sum_{i=1}^{N}\left(\frac{1}{\sin\phi_i}\right)$$

accounts for the shortening of the actual length of the pore as the intersection enlarges. If no new pore intersections are

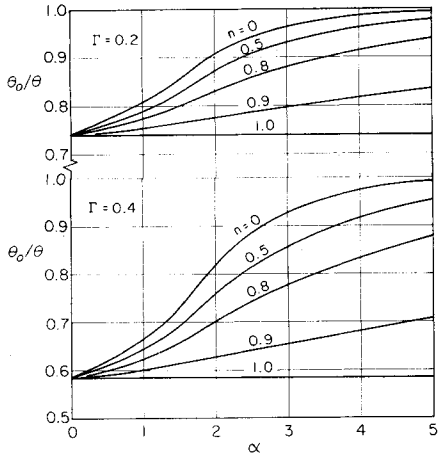

Fig. 6. Dependence of the reduced porosity on the parameter α at various reduced radii.

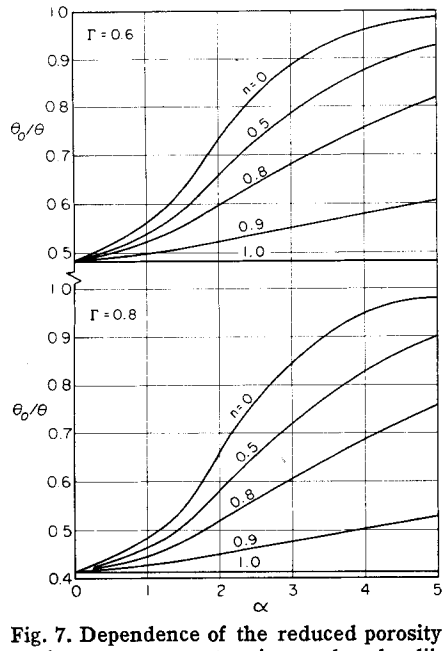

Fig. 7. Dependence of the reduced porosity on the parameter α at various reduced radii.

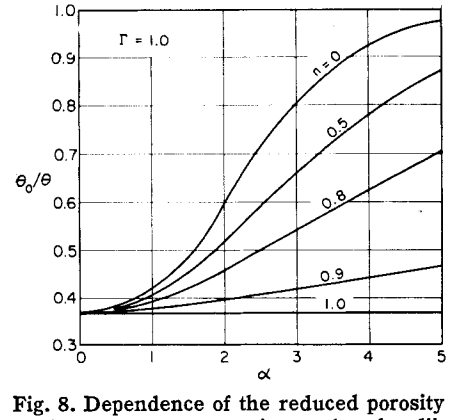

Fig. 8. Dependence of the reduced porosity on the parameter α at various reduced radii.

produced, the terms

$$\sum_{i=1}^{N}\left(\frac{1}{\sin\phi_i}\right) \quad \text{and} \quad \sum_{i=1}^{N}\beta(\phi_i)$$

are constant for a given solid and are abbreviated by A and B, respectively.

$$\therefore\ S = 2\pi r(L - Ar) - Br^2 \qquad (13)$$

$$\therefore \int_0^{\theta} d(\theta')$$

$$= \int_0^{r} [2\pi y(L - Ay) - By^2]\, dy \qquad (14)$$

$$\theta = L\pi r^2 - \left(\frac{2\pi A + B}{3}\right)r^3 \qquad (15)$$

$$\frac{\theta}{\theta_0} = \frac{\pi L r^2 - \left(\frac{2\pi a + B}{3}\right)r^3}{\pi L r_0^2 - \left(\frac{2\pi A + B}{3}\right)r_0^3} \qquad (16)$$

which reduces to

$$\frac{\theta}{\theta_0} = \xi^2\left(\frac{G - \xi}{G - 1}\right) \qquad (17)$$

where

$$G \equiv \frac{3\pi L}{r_0(2\pi A + B)}$$

To evaluate G, Equation (17) is assumed valid from $\theta = 0$ to $\theta = 1$. As $\theta \to 1$, $S \to 0$. Therefore

$$\frac{d\theta}{d\xi} = 2\xi\left(\frac{G - \xi}{G - 1}\right) - \xi^2\left(\frac{1}{G - 1}\right) \qquad (18)$$

$$\therefore \qquad 2(G - \xi) - \xi = 0$$

$$\xi = \frac{2G}{3} \qquad (19)$$

Substituting Equation (19) into Equation (17) and solving for G gives

$$G^3 - \frac{27}{4\theta_0}G + \frac{27}{4\theta_0} = 0 \qquad (20)$$

Many solids have porosities between 0.30 and 0.40. The particular samples for which data were available had an initial porosity θ_0 of 0.303. Using the value of $\theta_0 = 0.303$ in Equation (20) gives a value of $G = 4.105$. This value of G in Equation (17) gives the required relationship between θ and ξ.

In cylindrical coordinates Equations (1) and (2) become

$$\frac{\partial C}{\partial t} = \frac{D}{\theta R}\frac{\partial}{\partial R}\left(\theta R \frac{\partial C}{\partial R}\right) - akC \qquad (21)$$

$$\frac{\rho_s}{M\theta}\frac{d\theta}{dt} = kaC \qquad (22)$$

where a = the area per unit volume of pores. From Equations (17) and (18),

$$a = \frac{d\theta}{\theta r_0\, d\xi}$$

$$= \frac{(2G - 3\xi)}{r_0\xi(G - \xi)} \qquad (23)$$

In dimensionless form Equations (21) and (22) are

$$\frac{\partial\psi}{\partial\tau} = \frac{1}{\theta\eta}\frac{\partial}{\partial\eta}\left(\theta\eta\frac{\partial\psi}{\partial\eta}\right)$$

$$- \alpha^2\left(\frac{2G - 3\xi}{\xi(G - \xi)}\right)\psi \qquad (24)$$

and

$$\frac{d\xi}{d\tau} = \frac{\theta_0 M}{\rho_s}\alpha^2 C \qquad (25)$$

where

$$\alpha^2 = \frac{R_0^2 k}{r_0 D}, \quad \tau = \frac{Dt}{R_0^2}, \quad \xi = \frac{r}{r_0},$$

$$\eta = \frac{R}{R_0}, \quad \text{and} \quad \psi = \frac{C}{C_0}$$

The rate of reaction per unit length of sample at any time τ is

$$\Re(\tau) = -2\pi R_0\theta D\left(\frac{\partial C}{\partial R}\right)_{R_0}$$

$$= -2\pi\theta C_0 D\left(\frac{\partial\psi}{\partial\eta}\right)_{R_0=1} \qquad (26)$$

If the entire surface of the sample is available, the initial rate of reaction per unit length of sample is

$$\Re(0) = \frac{\pi R_0^2 k\theta_0(2G - 3)C_0}{r_0(G - 1)} \qquad (27)$$

Therefore

$$\frac{\Re(\tau, \alpha)}{\Re(0, 0)} = -\frac{2}{\alpha^2}\frac{\xi^2(G - \xi)}{2(G - 3)}\left(\frac{\partial\psi}{\partial\eta}\right)_{R_0=1} \qquad (28)$$

Numerical solutions to Equations (17), (24), (25), and (28) were obtained by the numerical method outlined earlier. The numerical results are shown in Figures 5 through 9 in terms α, τ, ξ, η and a new parameter Γ defined by

$$\Gamma \equiv \frac{\theta_0 M\alpha^2 C_0\tau}{\rho_s}$$

or

$$= \frac{\theta_0 M k C_0 t}{\rho_s r_0} \qquad (29)$$

From Equation (25) it is clear that Γ corresponds to the change in reduced pore radius at the pore mouth; i.e., at $\Gamma = 1.0$, the value of the pore radius at the pore mouth has doubled.

Figure 5 shows the concentration profiles as functions of α and Γ. The concentration profiles for $\Gamma = 0$ can be checked by an analytical solution, as this corresponds to cases where the pores are uniform and $\xi = 1$. The initial steady state concentration profiles are given by the solution to Equation (30) below.

$$\frac{d^2\psi}{d\eta^2} + \frac{1}{\eta}\frac{d\psi}{d\eta} - \beta^2\psi = 0 \qquad (30)$$

where

$$\beta^2 = \frac{\alpha^2(2G - 3)}{(G - 1)}$$

The solution to Equation (24) for the boundary conditions

$$\left.\frac{\partial\psi}{\partial\eta}\right|_{\eta=0} = 0$$

and $\psi(1) = 1$ is

$$\psi = \frac{J_0(i\beta\eta)}{J_0(i\beta)} \qquad (31)$$

Values of the center-line concentration obtained numerically and from Equation (31) agree to within 1% for the values of α reported.

The extent of reaction at various depths within cylindrical samples, represented by the porosity ratio θ_0/θ, is shown in Figures 6, 7, and 8 as a function of Γ and α. The integral rates of reaction $\mathcal{R}(\tau)$, i.e., the summation of the point values of reaction over the solid, are given in Figure 9 in terms of Γ, α, and $\mathcal{R}(0)$. In the range of Γ from 0 to 1, the integral reaction rate goes through a maximum for values of α up to 4. Values of the relative reaction can be computed analytically for the case of $\Gamma = 0$ by differentiating Equation (31) in placing the value of the gradient at $\eta = 1$ in Equation (28). The relative rate becomes

$$\frac{\mathcal{R}(0, \alpha)}{\mathcal{R}(0, 0)} = \frac{2}{\beta} \frac{iJ_1(i\beta)}{J_0(i\beta)} \qquad (32)$$

The relative rates obtained numerically and from Equation (32) agree to within 0.6% for the values of α reported.

The equations and method of solution presented herein can be used to interpret the reaction between a porous solid and a gaseous reactant where the kinetic expression is or can be reduced to a linear function of concentration. The particular set of numerical results presented in Figures 5 through 9 is limited to solids having initial porosity of 0.3.

ILLUSTRATIVE EXAMPLE

The computed results based on the pellet model can be used to interpret the experiments of Petersen and Wright (*5*) on the gasification of graphite at 1,100°C. with carbon dioxide at 1 atm. pressure. Rao (*6*) further studied the graphite–carbon dioxide reaction under conditions similar to those used by these workers. According to his results the reaction appeared to follow closely first-order kinetics with respect to carbon dioxide concentration and showed no poisoning effects by carbon monoxide under these conditions. Figure 10 summarizes the bulk-density-profile measurements made on 2- by ½-in.-diameter rod samples (*5*) reacted to weight losses of 0.63, 1, 2 and 3.26 g. in 29, 47, 86 and 129 min. of reaction time, respectively. The curves of Figure 10 are extrapolated to θ_0/θ at $\eta = 1$ and converted to values of ξ at the pore mouths by use of Equation (17). Figure 11 shows values of ξ vs. t. It will be observed that the relationship is nonlinear and in this respect does not correspond to the model assumed. If Equation (25) is rearranged, the slope of this plot can be related to the intrinsic reactivity and several constants:

$$\frac{d\xi}{dt} = \frac{\theta_0 M}{\rho_s} \frac{k}{r_0} C_0 \qquad (33)$$

where $\psi = 1$ at the pore mouth. Accordingly, the intrinsic reactivity k at the pore mouth can be computed from the slope of ξ vs. t curve in Figure 11. The variation of k can be independently estimated by selecting the value of α which most satisfactorily correlates the measured bulk-density curves and assuming that the diffusivity is constant. The latter method is only approximate because the numerical solutions to the differential equations are based upon α remaining constant during the integration. The value of α should be selected by matching curves near $\eta = 1$ and should give a predicted bulk-density profile lying slightly below the experimental line. Relative values of k were computed by the two methods given above at four values of the reaction time, and the methods agreed to within about 10%.

The magnitude of the effective diffusivity D_{eff} can be estimated from the α and k/r_0. After 47 min. of reaction time

$$\left(\frac{d\xi}{dt}\right)_{n=1} = 0.0054 \text{ min}^{-1}$$

and

$$\frac{k}{r_0} = \frac{\rho_s}{M\theta_0 C_0}\left(\frac{d\xi}{dt}\right)_{n=1}$$

$$= \frac{(2.22)(22{,}414)(1373)(0.0054)}{(12.01)(0.303)(273)(60)}$$

$$= 6.20 \text{ sec}^{-1}$$

The corresponding value of α is about 4.3; therefore

$$D_{eff} = \frac{R_0^2 k}{\alpha^2 r_0}$$

$$= \frac{(2.54)^2(6.2)}{(4)\ (4.3)^2}$$

$$= 0.135 \text{ sq. cm./sec.}$$

The magnitude of D_{eff} computed by this method does not compare favorably with bulk diffusivity D_B of 2.13 sq. cm./sec. calculated by the method given by Hirschfelder, Curtiss and Bird (*1*) for the CO_2–CO system at 1,373°K. Small values of the ratio D_{eff}/D_B have been reported in the literature. Hoogschagen (*2*) discusses values of this ratio obtained from his own experiments as well as those from other investigators. Walker and coworkers (*8*) reported an experimental value of D_{eff} equal to 0.046 sq. cm./sec. (at standard temperature and pressure) for similar graphite material in a system containing an H_2–N_2 mixture. From this experimental value one can estimate the D_{eff} for the CO_2–CO system at 1,373°K. by the ratio of D_B for the CO_2–CO system at 1,373°K. to D_B of the H_2–N_2 system at standard temperature and pressure. The estimated D_{eff} is therefore 0.145 sq. cm./sec., which is very close to the value obtained in this work.

A somewhat higher value of D_{eff} can be obtained if a "tortuosity factor" is included in the definition of α to allow for the fact that the axes of pores are not perpendicular to cylinder axis. The latter is assumed when R is used as an independent variable in Equation (21). The inclusion of a tortuosity factor ζ would change this variable to ζR. Values of ζ greater than 2 are difficult to justify on theoretical grounds. If a tortuosity factor had been used in this analysis, the D_{eff} calculated would be increased by a factor of ζ^2.

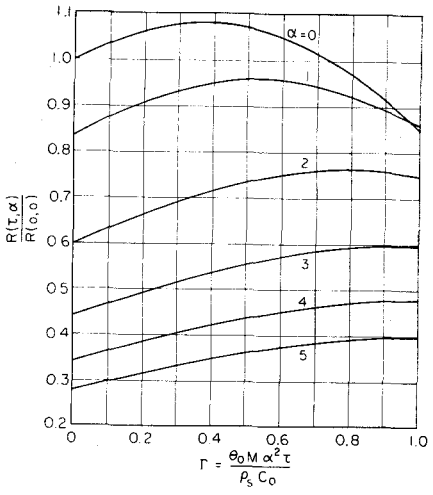

Fig. 9. Relative reaction rates as a function of time for various values of the parameter α for porous-solid model.

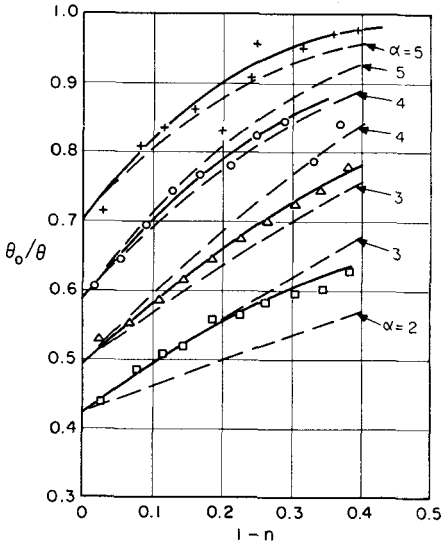

Fig. 10. Comparison of reduced porosity profiles computed from porous-solid model with those experimentally measured for the reaction of graphite rods with carbon dioxide at 1,100°C.

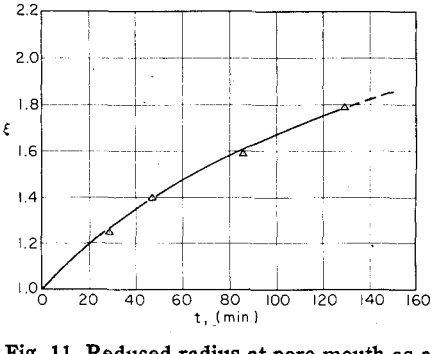

Fig. 11. Reduced radius at pore mouth as a function of time for reaction between graphite rods and carbon dioxide at 1,100°C.

It is unlikely that the low value of D_{eff} can be attributed to Knudsen-type flow because the mean pore radius in the unreacted samples is about 2 μ, with the majority of the pore radii in the range of 0.5 to 4 μ (4).

The low magnitude of the D_{eff} computed from the α and k/r_0 can probably best be explained by reexamining how well the structural features of the model and sample correspond. The graphite rods are made from ground petroleum coke particles with a rather large range of particle sizes (4), which are bound together with coal-tar pitch and heat treated at very high temperatures. The pores of this material are made up of interstitial spaces between particles and vary in "diameter" and shape. In the replacement of this system by an "equivalent" system of uniform cylindrical pores characterized by an average diameter, it is not surprising that the diffusivity necessary to give the correct rate of mass transport is much smaller than the bulk diffusion coefficient normally calculated at the temperature and pressure at which the experiment is carried out.

The integral reaction rates can be calculated from Figure 9 and compared with the experimental value. After 47 min. of reaction time the integral reaction rate of the graphite samples was 1.53 g./hr. According to Equation (27), if the entire sample surface had been available the rate of reaction would have been 7.75 g./hr. From Figure 9 $\Re(\tau)/\Re(0) = 0.4$ at values of $\Gamma = 0.4$ and $\alpha = 4.3$. If a correction is made to allow for the variation of k with reaction, the predicted rate for this sample is

$$\Re(\tau) = \frac{(7.75)(0.0054)(0.4)}{(0.01)} = 1.66\,\text{g./hr.}$$

where the values of 0.0054 and 0.01 are proportional to k at 47 and 0 min., respectively. The agreement between the estimated and observed rates is satisfactory.

SUMMARY

The method used in this paper to solve the differential equation for simultaneous diffusion and chemical reaction can be applied to systems where the kinetic term is linear in concentration. The numerical results presented herein are valid for materials with an initial uniform porosity of 0.3. The interpretation of the experimental gasification results between graphite and carbon dioxide making use of the pore model described in this paper indicates that the value of the effective diffusivity is an order of magnitude lower than the corresponding bulk diffusivity calculated at the same temperature and pressure. This low value of the effective diffusivity will probably be obtained whenever the real pore system containing pores of varying "diameters" is replaced by an idealized system of uniform, cylindrical pores characterized by an average diameter.

ACKNOWLEDGMENT

The author wishes to express his appreciation to Dr. Theodore Vermeulen and Dr. Andreas Acrivos for their helpful discussions concerning this work.

APPENDIX I

For very short reaction times, Equation (4) reduces to

$$\frac{\partial \psi}{\partial \tau} = \frac{\partial^2 \psi}{\partial \eta^2} - \alpha^2 \psi \qquad (34)$$

where $\xi \approx 1$. The solution to Equation (34) can be compared to the corresponding steady state solution, and if the concentration at a depth L within the pore approaches the steady state value before appreciable increase in ξ occurs at the pore mouth, then the solution based upon a series of secular steady state concentration profiles is a close approximation of the solution to unsteady state partial-differential equations.

The solution to Equation (34) at $\eta = 1$, for the boundary conditions given in Equation (7) and the initial condition that $\psi = 0$ for all η at $\tau = 0$ is given by

$$\psi(\tau, \eta) = \frac{\cosh\{\alpha(1-\eta)\}}{\cosh\alpha} - \frac{4}{\pi}\sum_{n=0}^{\infty} \frac{(-1)^n \exp\left\{-\left[\frac{\alpha^2 - (2n+1)^2\pi^2}{4}\right]\tau\right\} \cos\left\{\frac{(2n+1)(1-\eta)\pi}{2}\right\}}{(2n+1)\left[1 + \frac{4}{(2n+1)^2\pi^2}\right]} \qquad (35)$$

The corresponding steady state equation is

$$\psi(\infty, n) = \frac{\cosh\{\alpha(1-\eta)\}}{\cosh\alpha} \qquad (36)$$

The fractional approach to steady state at some time τ is given by the quotient of Equations (35) and (36), which for the case of $\alpha = 1$, $\eta = 1$, and $\tau = 10$, reduces to

$$\frac{\psi(10, 1)}{\psi(\infty, 1)} = 0.99999$$

However, during the interval $\tau = 10$, the fractional change in $\Delta\xi$ at the pore mouth as given by Equation (5) is

$$\frac{\Delta\xi}{\xi} = \frac{M}{2\rho_s}(\alpha^2)C_0\psi(\Delta\tau) = \frac{(12.01)(1)(273)(10)}{(2)(2.22)(22{,}414)(1{,}373)} = 2.4 \times 10^{-4}$$

for the conditions of the graphite–carbon dioxide reaction used as an example in this paper. For $\alpha = 5$, $\psi(10, 1)/\psi(\infty, 1) = 0.999994$ and $\Delta\xi/\xi = 6 \times 10^{-3}$. Therefore, the secular steady state solutions presented in this paper are valid except for extremely high values of C_0 and M/ρ_s.

NOTATION

a = specific surface area, area per unit volume of pores
C = concentration of reactant
C_0 = concentration of reactant at pore mouth
D = diffusion coefficient
G = constant
k = intrinsic reactivity
L = half pore length
M = molecular weight
N = number of pore intersections per unit volume of solid
r_0 = initial pore radius
r = pore radius
R' = reaction rate per unit surface area
$\Re$ = integral reaction rate
s = surface area of sample per unit volume of solid
t = time
u = average bulk gas velocity in pores
x = distance from pore mouth

Greek Letters

α = dimensionless parameter, $L\sqrt{\frac{k}{r_0 D}}$ or $R_0\sqrt{\frac{k}{r_0 D}}$
β = constant
$\beta(\phi_i)$ = shape factor
Γ = dimensionless parameter, $\theta_0 M k C_0 t/\rho_s r_0$
ξ = reduced pore radius, r/r_0
η = reduced radius, R/R_0
ϕ_i = angle of intersection of ith pore
ψ = reduced concentration, C/C_0
θ = porosity
θ_0 = initial porosity
ρ_s = density of solid phase
ζ = "tortuosity factor"
σ = surface roughness
τ = reduced time, Dt/L^2 or Dt/R_0^2
J_0 = Bessels function of 1st kind, zero order
J_1 = Bessels function of 1st kind, first order
div = divergence operator
grad = gradient operator

LITERATURE CITED

1. Hirschfelder, J. O., C. F. Curtiss, and R. B. Bird, "Molecular Theory of Gases and Liquids," John Wiley and Sons, New York (1954).
2. Hoogschagen, Jan, *Ind. Eng. Chem.*, **47**, 906 (1955).
3. Michael, A. D., "Matrix and Tensor Calculus," John Wiley and Sons, New York (1947).
4. Petersen, E. E., *Ind. Eng. Chem.*, **47**, 1630 (1955).
5. ———, and C. C. Wright, *ibid.*, p. 1,624.
6. Rao, P. V. N. Ramachandra, M.S. thesis, Univ. Calif., Berkeley (1954).
7. Thiele, E. W., *Ind. Eng. Chem.*, **31**, 916 (1939).
8. Walker, P. L., Jr., Frank Rusinko, Jr., and Emile Raats, *J. Phys. Chem.*, **59**, 245 (1955).
9. Weisz, P. B., and C. D. Prator, "Advances in Catalysis," vol. VI, Academic Press, Inc., New York (1954).
10. Wheeler, A., *ibid.*, vol. III (1951).